# An AP-1/clathrin coat plays a novel and essential role in forming the Weibel-Palade bodies of endothelial cells

Winnie W.Y. Lui-Roberts, Lucy M. Collinson, Lindsay J. Hewlett, Grégoire Michaux, and Daniel F. Cutler

Medical Research Council Laboratory of Molecular Cell Biology, Cell Biology Unit and Department of Biochemistry and Molecular Biology, University College London, London, WC1E 6BT, England, UK

Clathrin provides an external scaffold to form small 50–100-nm transport vesicles. In contrast, formation of much larger dense-cored secretory granules is driven by selective aggregation of internal cargo at the trans-Golgi network; the only known role of clathrin in dense-cored secretory granules formation is to remove missorted proteins by small, coated vesicles during maturation of these spherical organelles. The formation of Weibel-Palade bodies (WPBs) is also cargo driven, but these are cigar-shaped organelles up to 5 μm long. We hypothesized that a cytoplasmic coat might be required to make these very different structures, and we found that new and forming WPBs are extensively, sometimes completely, coated. Overexpression of an AP-180 truncation mutant that prevents clathrin coat formation or reduced AP-1 expression by small interfering RNA both block WPB formation. We propose that, in contrast to other secretory granules, cargo aggregation alone is not sufficient to form immature WPBs and that an external scaffold that contains AP-1 and clathrin is essential.

## Introduction

Weibel-Palade bodies (WPBs) are the large secretory organelles, which can be up to 5 μm long, of endothelial cells. They are uniquely "cigar-shaped"—typically cylindrical with hemispheric ends (Weibel and Palade, 1964; Wagner, 1990; Hannah et al., 2002; Michaux and Cutler, 2004). Their best understood components are the hemostatic protein von Willebrand factor (VWF; Sakariassen et al., 1979; Wagner et al., 1982; Sadler, 1998; Ruggeri, 1999) and the integral membrane protein P-selectin (Bonfanti et al., 1989; McEver et al., 1989). Regulated exocytosis of WPBs delivers VWF and P-selectin to the cell surface where they act in the recruitment of platelets and leukocytes. WPBs thus play a vital role in acute inflammation and in formation of the primary hemostatic plug. P-selectin–deficient mice have delayed neutrophil extravasation upon injury (Mayadas et al., 1993; Subramaniam et al., 1997), whereas the commonest inherited human bleeding disorder, von Willebrand's disease, largely results from mutations in VWF (Wagner, 1990; Nichols and Ginsburg, 1997; Sadler, 1998). The biogenesis of secretagogue-responsive WPBs is therefore of prime physiological importance, and their unusual shape has always implied that this process may be complex but little is known of the mechanisms involved.

Protein content is thought to play an important part in secretory granule biogenesis, driving the formation of these organelles by selective aggregation at the TGN (for review see Thiele and Huttner, 1998) to form their dense proteinaceous core. One of the most dramatic demonstrations of cargo-driven biogenesis follows the heterologous expression of VWF, which triggers the formation of pseudo-WPBs in nonendothelial and, even, nonsecretory cells (for review see Michaux et al., 2003). Not only are the structures formed in this way indistinguishable from bona fide WPBs at the EM level, but they also recruit WPB-resident membrane proteins and undergo exocytosis in response to secretagogue stimulation.

Cytoplasmic coat complexes act structurally during formation of vesicles and also help select membrane and content proteins for inclusion. Clathrin and the clathrin-associated adaptor protein complex AP-1 have been reported to act on immature secretory granules (ISGs) during granule maturation. In rat endocrine pancreatic β cells, AP-1/clathrin-coated vesicles (CCVs) remove missorted mannose 6-phosphate receptors

Correspondence to D.F. Cutler: d.cutler@ucl.ac.uk

L.J. Hewlett's present address is Division of Molecular Neuroendocrinology, National Institute for Medical Research, London, NW7 1AA, England, UK.

Abbreviations used in this paper: BFA, brefeldin A; CCV, clathrin-coated vesicle; HEK, human embryonic kidney; HUVEC, human umbilical vein endothelial cell; ISG, immature secretory granule; RNAi, RNA interference; siRNA, small interfering RNA; ssHRP, signal sequence HRP; VWF, von Willebrand factor; WPB, Weibel-Palade body.

The online version of this article includes supplemental material.


The Journal of Cell Biology, Vol. 170, No. 4, August 15, 2005 627–636
http://www.jcb.org/cgi/doi/10.1083/jcb.200503054

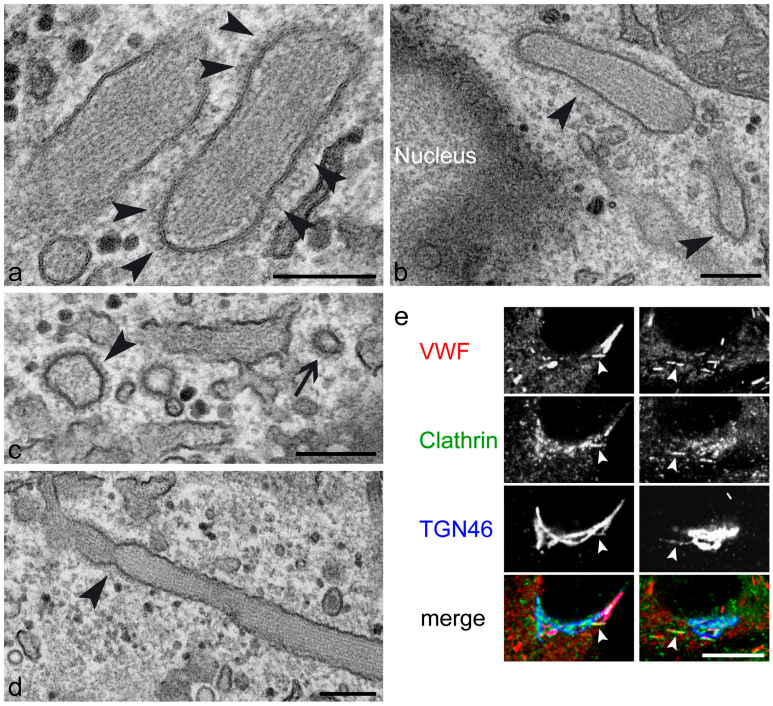


Figure 1. **Perinuclear WPBs are coated.** (a–d) Conventional transmission EM of HUVECs shows extensive coating of WPBs. Bars, 200 nm. (a) Arrowheads point to the coat covering a WPB. (b) Such coating is more often observed in the perinuclear region (arrowheads). (c) A transverse section of a WPB (arrowhead) and a typical CCV (arrow) have different diameters. (d) Partial coating (arrowhead) on a WPB is seen where the VWF tubules are less structured. (e) Newly emerging WPBs at the TGN (arrowheads) in two different cells partially colocalize with clathrin by immunofluorescence. Bar, 10 μm.

from ISGs (Klumperman et al., 1998). In neuroendocrine PC12 cells, the protein convertase furin and the mannose 6-phosphate receptor are also removed from ISGs via AP-1 CCVs (Dittie et al., 1999). The removal of missorted proteins and the gradual condensation of the protein content are major elements of the maturation of secretory granules (for reviews see Arvan and Castle, 1998; Tooze et al., 2001). Are AP-1 and clathrin involved in the formation of WPBs?

EM analysis of human umbilical vein endothelial cells (HUVECs) revealed extensive coating of newly formed and forming perinuclear WPBs. Coverage of WPBs by visible coats along the long axis for up to 650 nm and complete coating of WPBs up to 150 nm in diameter have been observed. We used immunofluorescence to show that this coat contains clathrin and AP-1, the latter further confirmed by immuno-EM. Reducing the ability of AP-1 and clathrin to function by anti–AP-1 RNA interference (RNAi) or a dominant-negative AP180 construct, which prevents the inclusion of clathrin into forming coats, does not, as might be expected from the previous work on secretory granules mentioned in the previous paragraph, lead to the accumulation of missorted proteins within WPBs, but instead to a failure to form WPBs at all. Our results provide the first evidence that coat proteins can also play an essential role in the initial formation of a secretory granule rather than only during their maturation.

## Results

### WPBs are coated

By conventional transmission EM of ultrathin sections from epon-embedded HUVECs, WPBs appear as cigar-shaped membrane-bound organelles with internal VWF tubules (striations in longitudinal sections) that make up the bulk of their content. Interestingly, we found that some WPBs are extensively, possibly even completely, covered with a proteinaceous coat (Fig. 1, a and b). The scale of the coverage is remarkable, given the size of WPBs. At least part of the coat has a bristle-like structure, resembling clathrin. Fig. 1 c shows a similar coat surrounding the transverse section of a small immature WPB (arrowhead), which was identified based on its size and the characteristic granular appearance of the content protein. VWF tubules are occasionally visible in transverse sections of WPBs (Fig. S3 a, available at http://www.jcb.org/cgi/content/full/jcb.200503054/DC1), depending on the angle of sectioning. The presence of a typical CCV (Fig. 1 c, arrow) within this section emphasizes by comparison the scale and extent of coating seen on WPBs. CCVs, including those involved in ISG maturation, are 50–100 nm in diameter. To cover the small WPBs in the top of Fig. 1 b, one would need at least 20 times more clathrin than is required to coat a conventional CCV. Immunofluorescence studies on HUVECs revealed partial colocalization of VWF and clathrin (Fig. 1 e) in structures that are clearly cigar shaped and that are associated with TGN46. The electron micrograph in Fig. 1 d shows a WPB with partial coating at an area where the VWF tubules are less structured. This might correspond to the VWF-containing structures (Fig. 1 e, right, arrowheads) that are partially coated with clathrin. The more extensive coating seen in the electron micrographs, as compared with the immunofluorescence, presumably reflects the use of glutaraldehyde in addition to PFA in the EM fixative. Our data suggests that at least some WPBs are completely covered, implying a structural role for this coat, rather than it simply being required to remove missorted proteins via conventional CCVs.

Our EM analyses also revealed that WPBs in the perinuclear part of the cell are more often coated than those in the pe-

riphery. Fig. 1 b shows two coated WPBs that are in close proximity to the nucleus. We previously showed that newly formed WPBs are found in this region, often as a distinctly located tangle of cigars, separated from the older, more generally distributed population (Hannah et al., 2003). This distribution for newly formed WPBs is in agreement with a TGN origin for these organelles, as are the cigar-shaped VWF-positive TGN46-positive structures that appear to be attenuated extensions of the TGN (Fig. 1 e, arrowheads). These observations suggest that the coat might play a role in the early stages of WPB formation.

The identification of clathrin on WPBs immediately raises the question of which specific coat components might be present. This is of importance both in its own right but also because the ability to manipulate a specific component of this coat in functional experiments (see the following section) reduces the possibility of any effects arising from an indirect effect of losing clathrin function, as clathrin is involved in multiple trafficking pathways. Immunofluorescence analyses of HUVECs reveal that AP-1 is found predominantly on perinuclear WPBs (Fig. 2, a–e), consistent with the EM localization of coated WPBs (Fig. 1). The AP-1 staining is present in patches along the whole length of the WPBs. We therefore postulate that the coat on WPBs may be labile and transient, in agreement with our need to increase levels of PFA in the fixative to 6% to obtain more consistent labeling. Immuno-EM of cryosections of HUVECs with anti–AP-1 and anti-VWF confirmed the presence of AP-1 on the surface of WPBs (Fig. 2, g and h, arrowheads). The relative size of coated WPBs (arrowheads) and CCVs (arrows) in Fig. 2 g is comparable with that in Fig. 1 c.

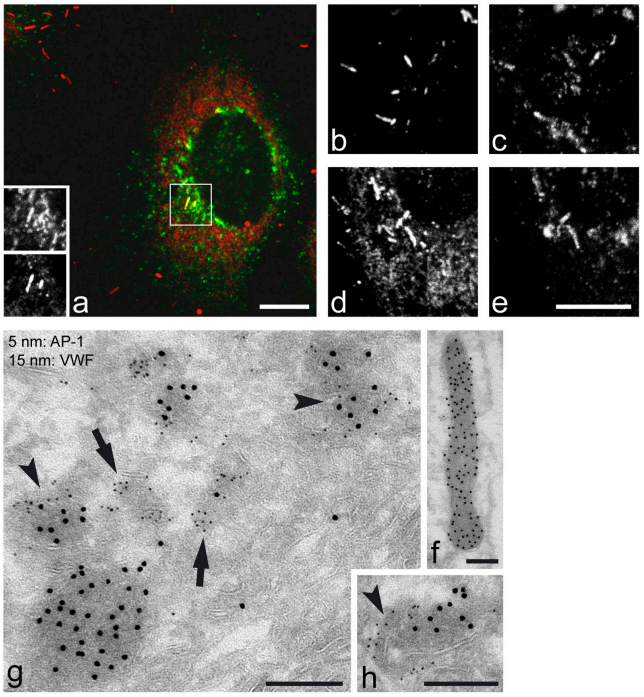


Figure 2. **AP-1 is present on WPBs.** (a–e) Partial colocalization of AP-1 and VWF shown by immunofluorescence. HUVECs were fixed in 6% PFA, permeabilized, and labeled with mouse anti–AP-1 and rabbit anti-VWF, followed by FITC-conjugated anti–mouse and Texas red–conjugated anti–rabbit secondary antibodies. Bars, 10 μm. (a) A perinuclear WPB is substantially covered with AP-1. The insets show a higher magnification of the boxed area (top inset, AP-1; bottom inset, VWF). (b–e) Further examples of partial colocalization of VWF (b and d) and AP-1 (c and e). (f–h) Immuno-EM of HUVEC cryosections show the presence of AP-1 on WPBs. Bars, 200 nm. (f) A WPB labeled with rabbit anti-VWF followed by 15 nm gold particles conjugated to protein A. (g) AP-1 is observed on CCVs (arrows) and it is also found at the rim of transverse sections of WPBs (arrowheads) near the Golgi. (h) An electron-dense coat that is labeled with an AP-1 antibody (arrowhead) is associated with an elongated VWF-containing structure.

## Clathrin and AP-1 are essential for WPB biogenesis

To study the role of clathrin and AP-1 in the formation of new WPBs, we expressed human full-length VWF in human embryonic kidney (HEK293) cells, which leads to the formation of pseudo-WPBs. These behave similarly to endothelial WPBs: they have a cigar-shaped structure and contain internal VWF tubules, recruit P-selectin, CD63, and Rab27a, and are capable of regulated secretion (Michaux et al., 2003). This model system enables us to avoid the possibility of preexisting WPBs masking any effects of our experiments on the formation of new WPBs and to carry out quantitative VWF secretion analyses without any background from WPBs made before manipulation.

To examine the role of clathrin in WPB formation, we reduced the functional pool of clathrin in HEK293 cells by expressing an AP180 construct (AP180-C; Ford et al., 2001) which contains a clathrin-binding domain and has a dominant-negative effect on clathrin function. If the only role of clathrin is to retrieve missorted proteins during the maturation of WPBs as in conventional ISG biogenesis (Introduction), we would expect to find immature WPBs containing mislocalized proteins in AP180-C/VWF–cotransfected HEK293 cells. Surprisingly, no cigar-shaped WPBs at all are found in these cells (Fig. 3, a and b) but instead VWF localized to fine puncta (Fig. 3 b). To examine the functional significance of this altered morphology, we examined the constitutive and secretagogue-stimulated release of VWF from VWF-expressing HEK293 cells that had been cotransfected with AP180-C or a control plasmid. The cells were rinsed and incubated in serum-free medium (serum contains VWF) without any secretagogue for 30 min, and then with medium containing the secretagogue PMA for 30 min further. Culture media were collected after each 30-min incubation and ELISA-based assays were performed for VWF quantification. The PMA-responsive pool of VWF was estimated by subtracting the amount of VWF released by constitutive secretion from that released upon PMA addition. The data were expressed as a percentage of the total VWF signal (see Materials and methods). In AP180-C–transfected HEK293 cells, we found a significant reduction in regulated secretion of VWF (Fig. 4 a). The increase in fine VWF-positive puncta (Fig. 3 b) correlating with the raised level of constitutive VWF secretion (Fig. 4 a) suggests that these might be constitutive secretory vesicles. Upon coexpression of VWF and AP180-C, some cells expressed VWF but not AP180-C, which may explain the small residual pool of PMA-responsive VWF.

To determine the functional significance of AP-1 in WPB biogenesis, we performed RNAi on HEK293 cells using a small

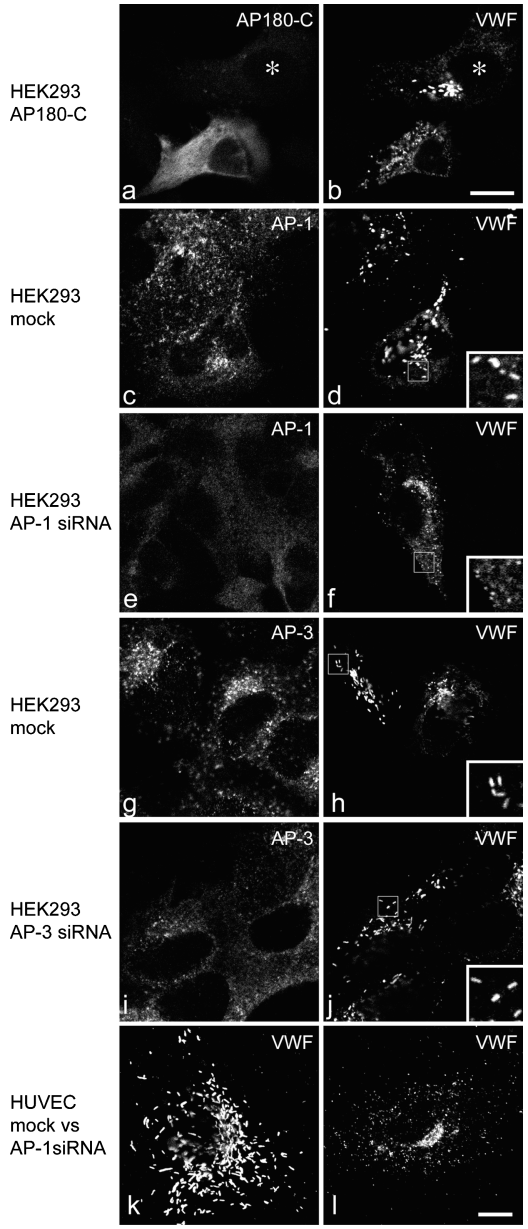


Figure 3. **Clathrin and AP-1 are required for WPB biogenesis.** (a and b) HEK293 cells were cotransfected with AP180-C and full-length VWF constructs. WPB formation was impaired in a cell transfected with AP180-C. In contrast, elongated WPBs were clearly seen in a cell that did not contain AP180-C (*). (c–j) The depletion of AP-1, but not AP-3, impairs the formation of WPBs in HEK293 cells. Cells were transfected with a full-length VWF construct and AP-1 siRNA (e and f), AP-3 siRNA (i and j), or mock transfected (c, d, g, and h). Although elongated WPBs were clearly observed upon AP-3 RNAi (j), WPBs formation was severely impaired upon AP-1 siRNA treatment (f). (k and l) Similar results were obtained in HUVECs. Elongated WPBs are abundant in a mock-treated cell (k) but not in the AP-1–depleted cell (l). Insets show a magnified view of the boxed regions. Bars, 10 μm.

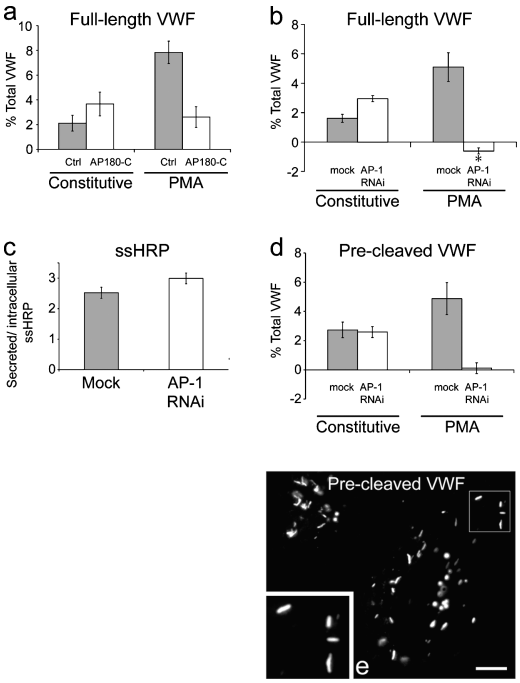


Figure 4. **AP180-C and AP-1 RNAi cause a significant reduction in PMA-stimulated VWF secretion, which is not the result from the loss of TGN integrity nor from furin missorting.** (a) HEK293 cells were cotransfected with a full-length VWF construct and AP180-C (white bars) or a control vector (gray bars). VWF secretion assays were performed 2–3 d after transfection. The PMA-responsive pool of VWF was estimated by subtracting the amount of VWF released from constitutive secretion from that released upon PMA addition. All data were normalized using the total signal of VWF (see Materials and methods). Each bar represents the mean ± SD, $n = 3$. (b and c) HEK293 cells were transfected with an siRNA targeted at the μ1 subunit of the AP-1 complex. After 3 d, the cells were further transfected with the same siRNA together with a full-length VWF construct (b) or an ssHRP construct (c). Secretion assays were performed 2–3 d after the second transfection. Although stimulated secretion of VWF was abolished, constitutive secretion of transfected ssHRP was not impaired in AP-1–depleted cells, suggesting the integrity of the TGN. The gray bars represent data from mock transfection, whereas the white bars represent data from the AP-1 RNAi. Each bar represents the mean ± SD, $n = 4$. *, see section Clathrin and AP-1 are essential for WPB biogenesis. (d) Cotransfection of the propeptide and mature VWF constructs failed to rescue the defect in regulated secretion in AP-1–depleted cells. Each bar represents the mean ± SD, $n = 5$. (e) Cotransfection with two VWF constructs containing the pro-region and the mature region, respectively, generated WPBs in control HEK293 cells. The cells were labeled with rabbit anti-VWF, followed by Texas red–conjugated donkey anti–rabbit secondary antibodies. Inset shows the magnified view of the boxed region. Bar, 10 μm.

interfering RNA (siRNA) against the μ1 subunit of the AP-1 complex (Hirst et al., 2003). Consistent with the fact that the incomplete AP-1 complex in μ1A-deficient cells cannot be recruited onto membranes (Meyer et al., 2000), the γ subunit of AP-1 became cytosolic when μ1 was knocked down by RNAi (Fig. 3 e). Two rounds of siRNA treatment were required for efficient knockdown, giving a knockdown level of ∼90%, as assessed by real-time PCR. As shown in Fig. 3 (e and f), AP-1 knockdown caused a failure in the formation of WPBs and was effectively a phenocopy of the effect of AP180-C transfection (Fig. 3 b), strongly suggesting that clathrin and AP-1 are involved in the same process. The specificity of the effect is illustrated by the fact that WPBs were still observed in VWF-transfected HEK293 cells (Fig. 3 j) when another clathrin-associated adaptor complex, AP-3, was depleted 90% by RNAi.

As with the AP180-C experiments, AP-1 knockdown caused an increase in the appearance of fine puncta in both HEK293 cells (Fig. 3 f) and HUVECs (Fig. 3 l). The latter also shows an example of the accumulation of VWF within pericen-

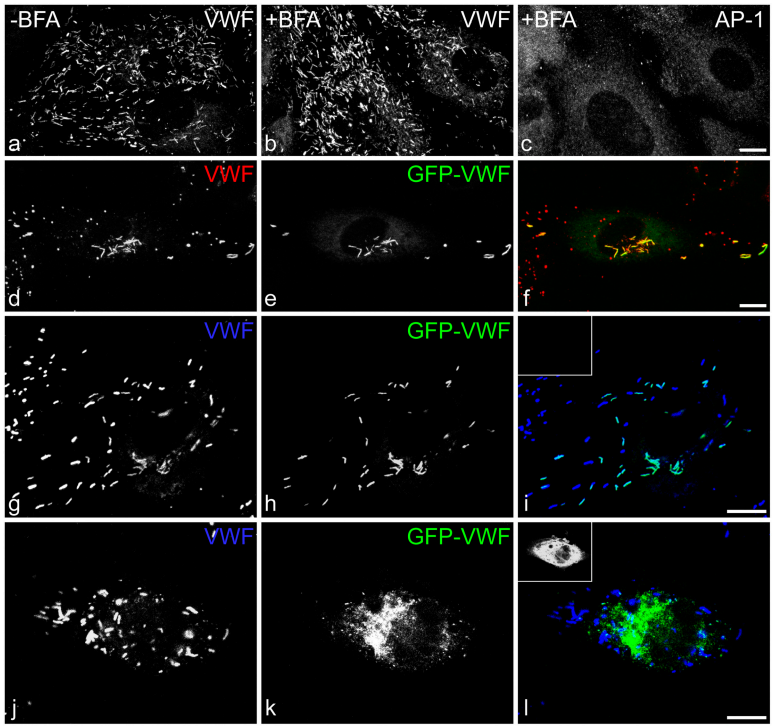


Figure 5. **The AP-1/clathrin coat is involved in an early stage of WPB biogenesis, but not in the maintenance of the cigar shape of preformed WPBs.** (a and b) A BFA-sensitive coat is not required for the maintenance of the shape of existing WPBs. HUVECs were treated with 5 μg/ml BFA for 30 min (b). Compared with untreated cells in panel a, there was no significant change to the appearance in anti-VWF staining. (c) Anti–γ-adaptin staining shows that AP-1 dissociates from WPBs and other membranes upon BFA treatment. (d–f) HUVECs were treated with 10 μM of monensin for 1 h (see Fig. S2), nucleofected with GFP-VWF, and allowed to recover overnight. The cells were labeled with rabbit anti-VWF (d), followed by Texas red–conjugated anti–rabbit antibody. Although the old rounded WPBs did not return to the original shape, newly synthesized WPBs had a classic rod shape (e). (g–l) HUVECs were microinjected with GFP-VWF together with a control vector plasmid (g–i) or AP180-C (j–l), fixed 16 h later, and labeled with anti-VWF (g and j; blue in i and l) and anti-GFP (h and k; green in i and l). Although old WPBs remained clearly visible in both cases, the cell microinjected with AP180-C failed to make new cigar-shaped WPBs. (insets) Anti-myc labeling shows the microinjected AP180-C construct. Bars, 10 μm.

triolar structures that is occasionally seen. ELISA-based VWF secretion assays in HEK293 showed that upon AP-1 RNAi, secretagogue-stimulated secretion of VWF was completely abolished (Fig. 4 b). This is in line with the failure of AP-1 knockdown cells to make WPBs. We also found that, as with the AP180-C experiments, there was an increase in constitutive secretion of VWF (Fig. 4 b). This increase may explain the negative value of stimulated VWF secretion in Fig. 4 b (asterisk), as it was calculated by subtracting the amount of VWF secreted constitutively from that secreted in a regulated manner. In summary, removal of clathrin or AP-1 by AP180-C expression or siRNA, respectively, gave rise to a very similar phenotype, suggesting that they work at the same step in WPB biogenesis.

### Defective WPB biogenesis does not reflect loss of TGN integrity nor furin missorting

When AP-1 was depleted, the regulated exocytosis of VWF was significantly reduced in parallel with the failure of WPB formation. However, the increase in constitutive secretion did not fully compensate for the drop in regulated secretion (Fig. 4 b). This raised the question of whether AP-1 depletion significantly affects the general structure of the TGN and impairs all the secretory pathways, thereby causing the failure in WPB formation. To test the functional integrity of the TGN, we cotransfected HEK293 cells with AP-1 siRNA and cDNA encoding the constitutive secretory marker signal sequence HRP (ssHRP; Connolly et al., 1994) and confirmed that the constitutive secretory pathway was not impaired (Fig. 4 c). In addition, we did not find a difference in the TGN at the light microscopy level by TGN46 immunolabeling in mock-transfected and AP-1–depleted HEK293 and HUVECs (Fig. S1, b–e, available at http://www.jcb.org/cgi/content/full/jcb.200503054/DC1). Our results therefore suggest that the TGN in AP-1–depleted cells remains fully capable of AP-1–independent functions. Consistent with our findings, it has been reported that cytosol depleted of ARF1, which is required for membrane recruitment of AP-1, is still able to support HA secretion in a permeabilized cell assay (Ellis et al., 2004). Together, we conclude that the failure of WPB formation in AP-1 knockdown cells is not caused by a general breakdown in TGN function.

As it passes through the trans-Golgi, pro-VWF is thought to be cleaved by furin to generate a propeptide of 741 aa and a mature protein of 2,050 aa (Creemers et al., 1993). Furin is localized to the TGN at steady state (for review see Thomas, 2002) but cycles through endosomes and the plasma membrane, and in μ1A-deficient fibroblasts, furin is missorted (Folsch et al., 2001) to endosomes. Indeed, we found that VWF cleavage was impaired in AP-1–depleted cells (Fig. S1 a). Whether furin cleavage is required for VWF storage in WPBs is not clear, as a VWF construct with a mutated furin cleavage site retains the ability to generate WPBs in CV-1 cells (Voorberg et al., 1993) but not in RIN5F cells (Journet et al., 1993). We find that there is an additional effect of AP-1 depletion independent of furin cleavage of VWF. We presented cells with a "pre-cleaved" form of VWF by coexpressing in trans the VWF propeptide and the mature VWF from separate constructs (Haberichter et al., 2000). As shown in Fig. 4 e, the coexpression of these two components results in normal WPB biogenesis (Haberichter et al., 2000; unpublished data). If the defect in WPB biogenesis that we observed in AP-1 knockdown cells is solely due to the missorting of furin, the precleaved VWF should rescue the wild-type VWF phenotype in Fig. 4 b. Importantly, the introduction of precleaved VWF did not rescue

the AP-1 knockdown phenotype (Fig. 4 d). The PMA-sensitive pool of VWF in AP-1 knockdown cells transfected with precleaved VWF remained negligible compared with that of the control cells. In addition, cell counting revealed that AP-1 knockdown on cells expressing precleaved VWF reduced the number of cells that contained cigar-shaped WPBs by threefold, and the number of WPBs in cells that had any WPBs at all was also reduced. Similarly, the precleaved VWF could not rescue the AP180-C phenotype (unpublished data). In conclusion, the defect in WPB biogenesis in AP-1 knockdown and AP180-C–transfected cells could not be simply explained by furin missorting. AP-1 and clathrin must therefore have an additional role in WPB biogenesis.

### Site of action and role of the coat

The localization of the clathrin/AP-1–coated WPBs and the fact that AP-1 knockdown and the overexpression of AP180-C abolish the formation of WPBs instead of affecting their maturation strongly suggest that the coat is acting to facilitate the initial formation of these organelles. To test if maintenance of the distinctive shape of existing WPBs is also coat dependent, we exploited the fact that a brief brefeldin A (BFA) treatment of cells causes ARF1-dependent coats, such as AP-1, AP-3, AP-4, and GGAs (Golgi-associated γ-ear-containing ARF-binding proteins), to dissociate from the membranes (Nie et al., 2003; Robinson, 2004). We tested whether a BFA-sensitive coat is required for maintaining the elongated shape of WPBs. HUVECs were treated with 5 μg/ml BFA for 2 min, after which the AP-1 complex was no longer membrane associated (Robinson and Kreis, 1992). There was no difference in the appearance of WPBs before and after BFA treatment, suggesting that, once a WPB is formed, the elongated shape can be maintained in the absence of a BFA-sensitive coat. Longer BFA incubations of 30 min also led to the same conclusion (Fig. 5, b and c).

Clathrin and AP-1 therefore appear to act early during the formation of WPBs. If the machinery of which these components are a part operates exclusively at an early stage of WPB biogenesis, then perturbation of WPB structure after budding from the TGN should be irreversible. We used monensin, an ionophore that perturbs the pH of organelles, to change the elongated WPBs to round structures (Fig. S2, available at http://www.jcb.org/cgi/content/full/jcb.200503054/DC1). Cells were then nucleofected with GFP-VWF and allowed to recover in monensin-free medium overnight (Fig. 5, d–f). The alteration in shape is irreversible because the rounded WPBs did not return to their original rod shape, whereas newly formed GFP-VWF–containing WPBs (Fig. 5 e) were a classic cigar shape. This result strongly implies that a critical event occurs during the initial stages of WPB biogenesis to form the elongated structure. Taking into account the prominence of coated WPBs in the perinuclear region and the effects of AP180-C and AP-1 RNAi on WPB biogenesis, we predict that clathrin and AP-1 are essential to the mechanism of this critical event that forms the cigar shape.

Our data suggest that although the clathrin/AP-1 coat is essential to the initial formation of WPB at the perinuclear region, it is not necessary to maintain the cigar shape once it is completely formed. As an independent confirmation of this, we microinjected HUVECs with a GFP-VWF construct to allow observation of the formation of new WPBs. At 16 h after microinjection, GFP-VWF expressed alone was clearly visible within cigar-shaped WPBs (Fig. 5 h). In 40 cells microinjected so as to express both AP180-C and GFP-VWF, we found no green WPBs but only fine puncta (Fig. 5 k), consistent with the results from HEK293 cells (Fig. 3 b). In this experiment, the accumulation of GFP-VWF is more obvious than in Fig. 3 b, probably due to the overexpression of GFP-VWF after microinjection. In this system, mature endogenous WPBs were identified by the presence of anti-VWF labeling coupled to a lack of GFP-VWF. In cells microinjected with AP180-C, mature elongated WPBs were still abundant (Fig. 5 j), confirming that clathrin is not required for the maintenance of WPBs, consistent with the BFA experiment (Fig. 5, a–c).

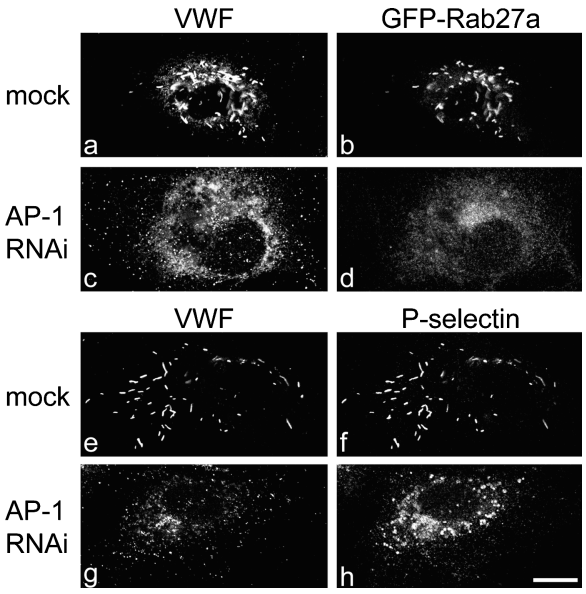


Figure 6. **VWF-positive puncta in AP-1–depleted HUVECs cannot recruit WPB components.** (a–d) GFP-Rab27a was recruited onto peripheral WPBs in mock-transfected cells (b), but upon AP-1 RNAi, became cytosolic (d) and failed to associate with the VWF-positive puncta (c). (e–h) HUVECs were treated with 100 μM leupeptin and 100 μM pepstatin for 6 h before fixation. The colocalization of P-selectin and VWF (e and f) was lost upon AP-1 RNAi (g and h). P-selectin was observed only after the lysosomal inhibitor treatment (h), suggesting that it was targeted to lysosomes for degradation in the absence of WPBs in AP-1–depleted cells. Bar, 10 μm.

### Failure in the recruitment of WPB components

AP-1–depleted cells lose the ability to generate elongated WPBs but generate fine VWF-positive puncta. These structures are not simply miniature WPBs because they do not have the ability to undergo regulated exocytosis. This loss suggests that they may also have an altered membrane composition. We therefore tested the ability of the VWF-positive puncta to recruit two WPBs membrane components, Rab27a and P-selectin. In AP-1–depleted HUVECs, GFP-Rab27a and P-selectin failed to be recruited onto the VWF-positive puncta (Fig. 6, d and h). GFP-Rab27a became cytosolic (Fig. 6 d), whereas

P-selectin was only observed after the addition of lysosomal inhibitors (Fig. 6 h), suggesting that it was delivered to endosomal/lysosomal compartments for degradation. Similar results were obtained in HEK293 cells (unpublished data). In contrast, VWF mutated such that it can no longer form cigar-shaped WPBs is still capable of recruiting these membrane proteins (Michaux et al., 2003). This implies a fundamental change in the VWF that is made in the absence of AP-1/clathrin.

## Discussion

We have discovered that WPBs are extensively coated. We have determined by EM and immunofluorescence that this coat includes clathrin and AP-1. We found that where coat function is experimentally prevented, cigar-shaped WPBs cannot be formed but that instead small VWF-positive puncta can be seen. Furthermore, there is a failure to recruit WPB membrane proteins and regulated secretion of VWF is significantly reduced. Interference with the ability of either clathrin or AP-1 to function has the same effect. Thus, we conclude that AP-1 and clathrin play a key role in a fundamental stage of WPB biogenesis.

There have been reports of extensive clathrin lattices on other intracellular organelles including stage I melanosomes (Raposo et al., 2001) and early vacuolar endosomes (Raiborg et al., 2001; Sachse et al., 2002). Melanosomes, like WPBs, are lysosome-related organelles, but not much is known about the coat on stage I melanosomes. The endosomal coat contains the clathrin-interacting protein Hrs (hepatocyte growth factor-regulated tyrosine kinase substrate), which binds, sequesters, and concentrates ubiquitinated receptors such as EGFR on the outer membrane of the endosomes (Raiborg et al., 2002; Sachse et al., 2002). However, unlike the endosomal coat, the coat on WPBs does not appear bilayered (Fig. 2 h). In addition, the endosomal coat does not contain AP-1 (Sachse et al., 2002), whereas GFP-Hrs does not localize to WPBs (unpublished data), suggesting different modes of action of these two clathrin coats.

### Coat function on WPBs

Clathrin and AP adaptor protein complexes mediate transport between subcellular compartments by forming small vesicular carriers. For instance, AP-2 CCVs are responsible for internalization of many receptors from the plasma membrane, whereas AP-1 CCVs are involved in vesicular transport between the TGN and endosomes. How does this relate to their appearance on a forming secretory granule at the TGN? Within forming WPBs, extra membrane has to be delivered as the WPB lengthens. The extensive coating could in principle somehow reflect the footprint of CCV delivering membrane to a forming WPB. This seems unlikely because new membrane is more likely to originate from within the TGN from which the WPB is budding, and also it has long been believed that CCVs have to be uncoated before they can fuse to target membranes (Ungewickell et al., 1995). Although a more recent study suggests that tubules partially coated with AP-1 may fuse with each other (Waguri et al., 2003) it does appear that a significant area of the fusion front is devoid of AP-1. Finally, judging by the degree of coating on WPBs in our electron micrographs, we conclude that it does not represent CCVs fused to WPBs because we would have to postulate that in addition to keeping their coat during fusion, the membrane would have to retain it after fusion.

By analogy to ISG formation (Dittie et al., 1997; Klumperman et al., 1998), we would expect that clathrin and AP-1 would participate in the retrieval of missorted proteins from immature WPBs. We have seen occasional coated budding profiles on WPBs by conventional EM (Fig. S3 b) that would be consistent with this maturation pathway. However, it is clear that this is not the sole function of coat proteins in WPB biogenesis because upon AP-1 RNAi we observed no WPBs rather than immature WPBs containing missorted proteins, indicating that WPB formation was blocked at an earlier stage. A more novel possibility is that the small budding profiles represent the removal of proteins or lipids that bend membranes, hereby contributing to the shaping of WPBs. However, a failure in this function should lead to the appearance of large, rounded WPBs. Finally, these buds might reflect the removal of channels or transporters that control the profolding milieu of the immature WPBs for VWF. That this environment is important is shown by the monensin data. However, a failure in such a function would also presumably lead to WPBs more like those seen after monensin, rather than the small puncta that we observed.

Another possible function of the coat that we considered was that the clathrin acts as a simple "corset" for WPBs; i.e., it facilitates the elongation of WPBs by acting as a mechanical shaping device during formation. This hypothesis derives from a simple consideration of the content of WPBs; i.e., the long proteinaceous tubules made from VWF that fill its interior. We wondered whether their parallel stacking along the long axis of the WPBs resulted from the constraining influence of a corset. However, this hypothesis, although attractive, is not consistent with the effects of losing the coat. Loss of a simple corset should lead to a large rotund WPBs (as produced by monensin treatment) rather than altogether losing the ability to bud a large VWF-positive structure.

In general, secretory granules form around their dense protein cores, which are made by selective aggregation within the TGN (Arvan and Castle, 1998; Tooze et al., 2001). The membranes of these roughly spherical organelles are not extensively coated and their biogenesis is seen as largely content driven; expression of granule content proteins can lead to the formation of dense-cored secretory granules de novo. Why are WPBs different? The most obvious difference between WPBs and conventional granules is that they are not round, but long cylinders. This structure is not likely to be a low-energy shape, and presumably requires some scaffolding to construct. We therefore propose a model in which the extensive coating somehow stabilizes the forming WPBs, perhaps allowing time for folding of its contents into the protein tubules characteristic of the WPBs, maybe even blocking its premature scission. The loss of such a scaffold would thus lead to a failure to make any object even closely resembling the WPBs, but instead to the formation of smaller puncta. Interestingly, although VWF secretion partially switches to constitutive release, not all of the protein does so. VWF is unusually able to drive the formation of

its own specialized carrier; even in cells with a regulated pathway, VWF is not targeted to the endogenous secretory granules but drives the formation of pseudo-WPBs instead (Wagner et al., 1991). It may therefore have an intrinsic tendency to avoid constitutive secretion. That losing the coat prevents the initial formation of the cigar strongly suggests that the coat is needed for allowing the contents to somehow drive the formation of its shape. This is supported by the results of the monensin experiment. We find that monensin treatment causes WPBs to become spherical, but that after removal of the drug, the treated WPBs cannot regain their cigar shape. This implies that shape formation is coupled to biogenesis, and thus to the coat because new WPBs form at the TGN where we see them coated.

The VWF-positive puncta in AP-1–depleted cells failed to recruit P-selectin or Rab27. Because it has been reported that P-selectin does not bind AP-1 (Daugherty et al., 2001), we speculate that the suggested prevention of premature scission by a scaffold provides more time for efficient recruitment of P-selectin and/or allows VWF to be processed to a configuration that somehow leads to the recruitment of membrane proteins. Because Rab27a is only recruited to mature WPBs (Hannah et al., 2003), the first mechanism is not possible for this protein. It should be noted that heterologous expression of VWF in HEK293 cells causes the recruitment of Rab27a, CD63, and P-selectin onto pseudo-WPBs (Michaux et al., 2003), suggesting that lumenal VWF can somehow drive the recruitment of proteins on the other side of the membrane.

In this paper, we present the first evidence that AP-1 and clathrin are essential to the initial steps of biogenesis of a regulated secretory organelle. AP-1 is known to interact with several accessory proteins, such as γ-synergin and epsinR (Page et al., 1999; Kalthoff et al., 2002; Wasiak et al., 2002; Hirst et al., 2003; Mills et al., 2003). To form WPBs, it is possible that a different set of effectors, which remain to be identified, are required. Unlike other secretory granules, we show that cargo aggregation alone is not sufficient to form immature WPBs. We propose that the AP-1/clathrin coat forms a stabilizing scaffold that is essential to the formation of these very large organelles and is not acting in organelle formation via small vesicles. Therefore, we have unveiled a novel mode of action for this AP-1–associated clathrin coat.

## Materials and methods

### Chemicals and antibodies

All chemicals were purchased from Sigma-Aldrich or BDH unless otherwise stated. Rabbit antibody against the δ subunit of AP-3 and mouse mAb against VWF propeptide (239.1) were gifts of M.S. Robinson (Cambridge Institute for Medical Research, Cambridge, UK; Simpson et al., 1997) and S.L. Haberichter (Medical College of Wisconsin, Milwaukee, WI; Haberichter et al., 2000), respectively. mAbs against γ-adaptin (mAb 100/3) and AP180 were purchased from Sigma-Aldrich. Mouse monoclonal anti-clathrin (clone X22) and anti-myc (9E10) were purchased from Abcam and Santa Cruz Biotechnology, Inc., respectively. Rabbit polyclonal anti-VWF and its HRP-conjugated form were obtained from DakoCytomation. Sheep polyclonal anti-VWF and anti-TGN46 were supplied by Serotec. Texas red–, FITC-, and Cy5-conjugated secondary antibodies were purchased from The Jackson Laboratory.

### Expression vector constructs

The construct expressing the COOH terminus of AP180 (AP180-C) was a gift of H.T. McMahon (Medical Research Council Laboratory of Molecular Biology, Cambridge, UK; Ford et al., 2001). The full-length human VWF construct in pCI-neo (Michaux et al., 2003) and ssHRP construct (Connolly et al., 1994) have been described previously. The human VWF propeptide (VWFpp) and mature VWF construct (Δpro) constructs were gifts from S.L. Haberichter (Haberichter et al., 2000). GFP-VWF (Romani de Wit et al., 2003), GFP-Hrs (Urbe et al., 2003), and GFP-Rab27a (Hume et al., 2001) were provided by J. Voorberg and J.A. Van Mourik (Sanquin Research at CLB, , Amsterdam, Netherlands), S. Urbé (University of Liverpool, Liverpool, UK), and M.C. Seabra (Imperial College London, London, UK), respectively.

### EM

HUVECs were grown on 6-cm Petri dishes (for embedding pellets) or coverslips (for embedding en face) and processed for conventional EM as previously described (Michaux et al., 2003). In brief, the cells were fixed with 2% PFA/1.5% glutaraldehyde in 0.1 M sodium cacodylate buffer and then treated with 1% osmium tetroxide/ 1.5% potassium ferricyanide, followed by 1% tannic acid. The samples were processed for conventional embedding in epon. Ultrathin 60-nm sections were stained with lead citrate and observed with a transmission electron microscope (model Philips EM420; FEI UK).

For immuno-EM of cryosections, HUVECs were fixed with 4% PFA in 0.1 M sodium phosphate buffer, pH 7.4 (PB), for 30 min at 37°C. Cells were washed in PB, and excess aldehyde was quenched using 50 mM glycine/PB. Cells were embedded in 12% gelatin, cryoprotected in 2.3 M sucrose at 4°C overnight, and frozen in liquid nitrogen as previously described (Raposo et al., 1997). Ultrathin cryosections were cut using an Ultracut FCS microtome (Leica) and picked up in a 1:1 mixture of 2% methylcellulose and 2.3 M sucrose. Cells were single labeled with either a mAb against γ-adaptin (mAb100/3; Sigma-Aldrich) or a rabbit polyclonal antibody against VWF (DakoCytomation). Sections were quenched in 50 mM glycine/50 mM $NH_4Cl$, labeled with primary antibody in 1% BSA/0.5% BSA-C (Aurion), and detected with 10-nm gold particles conjugated to protein A (PAG; obtained from J.W. Slot, Utrecht University, Utrecht, Netherlands). Where the primary antibody was a monoclonal, a rabbit anti–mouse bridging antibody (DakoCytomation) was used before the PAG. Cells were also double labeled with anti–γ-adaptin followed by a rabbit anti–mouse bridging antibody and 5 nm PAG. 1% glutaraldehyde was used to prevent recognition of the intermediate antibody by the secondary gold, before quenching and labeling with anti-VWF and 15 nm PAG. All sections were contrast stained and supported in a mixture of methylcellulose and uranyl acetate before being imaged with a transmission electron microscope.

### Tissue culture and transfection

HEK293 cells were obtained from BD Biosciences and were maintained in α-MEM medium (GIBCO BRL) with glutamax, 10% FCS (Sigma-Aldrich), and 50 μg/ml gentamicin (GIBCO BRL). HUVECs were purchased from TCS-Cellworks and were grown in HUVEC growth medium, which contains M199 medium with Earle's modified salts (GIBCO BRL), 20% FCS, 10 U/ml heparin (Sigma-Aldrich), 30 μg/ml endothelial growth supplement (Sigma-Aldrich), and 50 μg/ml gentamicin as previously described (Arribas and Cutler, 2000). For the monensin treatment, HUVECs were incubated with 10 μM monensin in HUVEC growth medium for 1 h at 37°C. For the BFA treatment, HUVECs were treated with 5 μg/ml BFA for 2, 10, or 30 min at 37°C before being processed for immunofluorescence.

Nucleofection (Amaxa) was used to transfect DNA and siRNA into tissue culture cells, according to the supplier's instructions. Typical transfection rate is 30–70%. For microinjection, 0.1 μg/μl DNA was injected together with biotin-dextran into the nuclei of ∼50 cells over a period of 20 min.

### RNAi

The siRNA directed against the μ1 subunit of AP-1 has been described previously (Hirst et al., 2003). siRNA against the β3A subunit of AP-3 was purchased from QIAGEN and the target sequence is ATGGCTGATCTTGAAGGTTTA. Cells were transfected with 300–600 pmol of siRNA by nucleofection (Amaxa) using the nucleofection program A-23 for HEK293 or program U-01 for HUVECs. Typically, a 15-cm Petri dish of cells that are 70–80% confluent were used for four to six nucleofection reactions. Two reactions were plated onto each 9-cm Petri dish and incubated for 2–3 d at 37°C. The cells were then nucleofected again with 4 μg of a full-length VWF DNA construct (Michaux et al., 2003) and 150–300 pmol of siRNA, and incubated for 3 d before being processed for immunofluorescence and secretion assays.

### Immunofluorescence

Tissue culture cells grown on coverslips were fixed with 3% PFA, quenched, and permeabilized with 50 mM $NH_4Cl$ and 0.2% saponin.

After blocking in PGAS (PBS, 0.2% gelatin, 0.02% $NaN_3$, and 0.02% saponin), the cells were incubated with primary antibodies for 45 min, washed in PGAS, followed by a 45-min incubation with fluorophore-conjugated secondary antibodies. The coverslips were washed in PGAS and mounted with ProLong antifade reagent (Molecular Probes). The image in Fig. 4 e was acquired using an Orca CCD camera (Hamamatsu) and Improvision Openlab software through a 63× oil immersion lens (NA 1.4) on a microscope (model Axioskop; Carl Zeiss MicroImaging, Inc.). All other coverslips were examined at ambient temperature through a 60× oil immersion lens (NA 1.4) on a microscope (model Optiphot 2; Nikon) fitted with a confocal laser scanner (model MRC 1024; Bio-Rad Laboratories) unless stated otherwise. Lasersharp (Bio-Rad Laboratories) was the image acquisition program used; Adobe Photoshop 6.0.1 and Illustrator 10 were used to generate figures from digital images.

### Secretion assays

Stimulated VWF secretion in transfected HEK cells was performed as previously described (Michaux et al., 2003). Cells were rinsed in the release medium (α-MEM with glutamax, 10 mM Hepes, pH 7.4, and 0.2% BSA) and 1.5 ml of release medium was put in each well for the 30-min constitutive secretion. The cells were incubated with 1.5 ml of release medium containing 100 ng/ml PMA for 30 min of stimulated secretion at 37°C. Medium was collected after each 30-min incubation. The remaining VWF was released by cell lysis at 4°C for 30 min in the lysis medium (release medium containing 0.5% vol/vol Triton X-100, 1 mM EDTA, and protease inhibitors). The relative amounts of VWF were quantified by ELISA as described previously (Blagoveshchenskaya et al., 2002). The level of secretion was normalized by the total amount of VWF, which was calculated by adding all the signals from the constitutive and stimulated secretions as well as the remaining VWF after secretions.

For the ssHRP secretion assays in HEK293 cells, an ssHRP construct (Connolly et al., 1994) was cotransfected during the second round of siRNA nucleofection. 2 d after the nucleofection, the cells were rinsed twice with the normal HEK293 growth medium. 1.5 ml of medium was put in each well and constitutive secretion of ssHRP was allowed to occur for 6 h at 37°C. The cells were then lysed as described in the previous paragraph to release the intracellular ssHRP left behind. HRP activity was measured using an *o*-phenylenediamine assay in which 100 µl of sample was incubated with an equal volume of assay buffer (39.2 mM citric acid, 132.4 mM dibasic sodium phosphate, 0.1% vol/vol Triton X-100, 0.1% vol/vol $H_2O_2$, and 0.6% vol/vol saturated *o*-phenylenediamine) for 15 min at RT in a 96-well plate. The reaction was stopped by adding 50 µl of 3 M HCl and the plate was read at 490 nm. The data were expressed as a ratio of constitutively secreted to intracellular ssHRP.

### Real-time PCR

RNA was prepared from tissue culture cells using QIAshredder (QIAGEN) and RNeasy mini kit (QIAGEN) according to the manufacturer's instructions. The RNA was then subjected to reverse transcription using SuperScript III first-strand cDNA synthesis system (Invitrogen). Real-time PCR was carried out in a DNA Engine Opticon 2 system (MJ Research) using DyNAmo SYBR green qPCR kit (Finnzymes). The C(T) data were normalized with a GAPDH internal control and analyzed using the $2^{-\Delta\Delta C(T)}$ method (Livak and Schmittgen, 2001). The primers used for GAPDH amplification were 5′-CAGCCTCAAGATCATCAGCA-3′ and 5′-GTCTTCTGGGTGGCAGTGAT-3′. For µ1 PCR, the primers 5′-CTAGTGTGGAGGCCGAAGAC-3′ and 5′-CGGAGCTGGTAATCTCCATT-3′ were used.

### Online supplemental material

Fig. S1 shows the impaired VWF cleavage and intact TGN morphology in AP-1–depleted cells, whereas Fig. S2 shows the effect of monensin on the shape of WPBs. Additional electron micrographs of WPBs can be found in Fig. S3. The online supplemental material is available at http://www.jcb.org/cgi/content/full/jcb.200503054/DC1.

We would like to express our gratitude to H.T. McMahon, S.L. Haberichter, J. Voorberg, J.A. Van Mourik, M.C. Seabra, S. Urbé, and M.S. Robinson for reagents. We also thank M.S. Robinson, C.E. Futter, M.N.J. Seaman, M. Deneka, and members of the Cutler laboratory for reading the manuscript and for helpful discussions.

This project was funded by the Medical Research Council (UK).

Submitted: 10 March 2005
Accepted: 7 July 2005

## References

Arribas, M., and D.F. Cutler. 2000. Weibel-Palade body membrane proteins exhibit differential trafficking after exocytosis in endothelial cells. *Traffic.* 1:783–793.

Arvan, P., and D. Castle. 1998. Sorting and storage during secretory granule biogenesis: looking backward and looking forward. *Biochem. J.* 332:593–610.

Blagoveshchenskaya, A.D., M.J. Hannah, S. Allen, and D.F. Cutler. 2002. Selective and signal-dependent recruitment of membrane proteins to secretory granules formed by heterologously expressed von Willebrand factor. *Mol. Biol. Cell.* 13:1582–1593.

Bonfanti, R., B.C. Furie, B. Furie, and D.D. Wagner. 1989. PADGEM (GMP140) is a component of Weibel-Palade bodies of human endothelial cells. *Blood.* 73:1109–1112.

Connolly, C.N., C.E. Futter, A. Gibson, C.R. Hopkins, and D.F. Cutler. 1994. Transport into and out of the Golgi complex studied by transfecting cells with cDNAs encoding horseradish peroxidase. *J. Cell Biol.* 127:641–652.

Creemers, J.W., R.J. Siezen, A.J. Roebroek, T.A. Ayoubi, D. Huylebroeck, and W.J. Van de Ven. 1993. Modulation of furin-mediated proprotein processing activity by site-directed mutagenesis. *J. Biol. Chem.* 268:21826–21834.

Daugherty, B.L., K.S. Straley, J.M. Sanders, J.W. Phillips, M. Disdier, R.P. McEver, and S.A. Green. 2001. AP-3 adaptor functions in targeting P-selectin to secretory granules in endothelial cells. *Traffic.* 2:406–413.

Dittie, A.S., L. Thomas, G. Thomas, and S.A. Tooze. 1997. Interaction of furin in immature secretory granules from neuroendocrine cells with the AP-1 adaptor complex is modulated by casein kinase II phosphorylation. *EMBO J.* 16:4859–4870.

Dittie, A.S., J. Klumperman, and S.A. Tooze. 1999. Differential distribution of mannose-6-phosphate receptors and furin in immature secretory granules. *J. Cell Sci.* 112:3955–3966.

Ellis, M.A., M.T. Miedel, C.J. Guerriero, and O.A. Weisz. 2004. ADP-ribosylation factor 1-independent protein sorting and export from the trans-Golgi network. *J. Biol. Chem.* 279:52735–52743.

Folsch, H., M. Pypaert, P. Schu, and I. Mellman. 2001. Distribution and function of AP-1 clathrin adaptor complexes in polarized epithelial cells. *J. Cell Biol.* 152:595–606.

Ford, M.G., B.M. Pearse, M.K. Higgins, Y. Vallis, D.J. Owen, A. Gibson, C.R. Hopkins, P.R. Evans, and H.T. McMahon. 2001. Simultaneous binding of PtdIns(4,5)P2 and clathrin by AP180 in the nucleation of clathrin lattices on membranes. *Science.* 291:1051–1055.

Haberichter, S.L., S.A. Fahs, and R.R. Montgomery. 2000. von Willebrand factor storage and multimerization: 2 independent intracellular processes. *Blood.* 96:1808–1815.

Hannah, M.J., R. Williams, J. Kaur, L.J. Hewlett, and D.F. Cutler. 2002. Biogenesis of Weibel-Palade bodies. *Semin. Cell Dev. Biol.* 13:313–324.

Hannah, M.J., A.N. Hume, M. Arribas, R. Williams, L.J. Hewlett, M.C. Seabra, and D.F. Cutler. 2003. Weibel-Palade bodies recruit Rab27 by a content-driven, maturation-dependent mechanism that is independent of cell type. *J. Cell Sci.* 116:3939–3948.

Hirst, J., A. Motley, K. Harasaki, S.Y. Peak Chew, and M.S. Robinson. 2003. EpsinR: an ENTH domain-containing protein that interacts with AP-1. *Mol. Biol. Cell.* 14:625–641.

Hume, A.N., L.M. Collinson, A. Rapak, A.Q. Gomes, C.R. Hopkins, and M.C. Seabra. 2001. Rab27a regulates the peripheral distribution of melanosomes in melanocytes. *J. Cell Biol.* 152:795–808.

Journet, A.M., S. Saffaripour, E.M. Cramer, D. Tenza, and D.D. Wagner. 1993. von Willebrand factor storage requires intact prosequence cleavage site. *Eur. J. Cell Biol.* 60:31–41.

Kalthoff, C., S. Groos, R. Kohl, S. Mahrhold, and E.J. Ungewickell. 2002. Clint: a novel clathrin-binding ENTH-domain protein at the Golgi. *Mol. Biol. Cell.* 13:4060–4073.

Klumperman, J., R. Kuliawat, J.M. Griffith, H.J. Geuze, and P. Arvan. 1998. Mannose 6-phosphate receptors are sorted from immature secretory granules via adaptor protein AP-1, clathrin, and syntaxin 6-positive vesicles. *J. Cell Biol.* 141:359–371.

Livak, K.J., and T.D. Schmittgen. 2001. Analysis of relative gene expression data using real-time quantitative PCR and the 2(-Delta Delta C(T)) method. *Methods.* 25:402–408.

Mayadas, T.N., R.C. Johnson, H. Rayburn, R.O. Hynes, and D.D. Wagner. 1993. Leukocyte rolling and extravasation are severely compromised in P selectin-deficient mice. *Cell.* 74:541–554.

McEver, R.P., J.H. Beckstead, K.L. Moore, L. Marshall-Carlson, and D.F. Bainton. 1989. GMP-140, a platelet alpha-granule membrane protein, is also synthesized by vascular endothelial cells and is localized in Weibel-Palade bodies. *J. Clin. Invest.* 84:92–99.

Meyer, C., D. Zizioli, S. Lausmann, E.L. Eskelinen, J. Hamann, P. Saftig, K. von Figura, and P. Schu. 2000. mu1A-adaptin-deficient mice: lethality,

loss of AP-1 binding and rerouting of mannose 6-phosphate receptors. *EMBO J.* 19:2193–2203.

Michaux, G., and D.F. Cutler. 2004. How to roll an endothelial cigar: the biogenesis of Weibel-Palade bodies. *Traffic.* 5:69–78.

Michaux, G., L.J. Hewlett, S.L. Messenger, A.C. Goodeve, I.R. Peake, M.E. Daly, and D.F. Cutler. 2003. Analysis of intracellular storage and regulated secretion of 3 von Willebrand disease-causing variants of von Willebrand factor. *Blood.* 102:2452–2458.

Mills, I.G., G.J. Praefcke, Y. Vallis, B.J. Peter, L.E. Olesen, J.L. Gallop, P.J. Butler, P.R. Evans, and H.T. McMahon. 2003. EpsinR: an AP1/clathrin interacting protein involved in vesicle trafficking. *J. Cell Biol.* 160:213–222.

Nichols, W.C., and D. Ginsburg. 1997. von Willebrand disease. *Medicine (Baltimore).* 76:1–20.

Nie, Z., D.S. Hirsch, and P.A. Randazzo. 2003. Arf and its many interactors. *Curr. Opin. Cell Biol.* 15:396–404.

Page, L.J., P.J. Sowerby, W.W. Lui, and M.S. Robinson. 1999. γ-Synergin: an EH domain–containing protein that interacts with γ-adaptin. *J. Cell Biol.* 146:993–1004.

Raiborg, C., K.G. Bache, A. Mehlum, E. Stang, and H. Stenmark. 2001. Hrs recruits clathrin to early endosomes. *EMBO J.* 20:5008–5021.

Raiborg, C., K.G. Bache, D.J. Gillooly, I.H. Madshus, E. Stang, and H. Stenmark. 2002. Hrs sorts ubiquitinated proteins into clathrin-coated microdomains of early endosomes. *Nat. Cell Biol.* 4:394–398.

Raposo, G., M.J. Kleijmeer, G. Posthuma, J.W. Slot, and H.J. Geuze. 1997. Immunogold labeling of ultrathin cryosections: application in immunology. *In* Handbook of Experimental Immunology. L.A. Herzenberg, D.M. Weir, and C. Blackwell, editors. Blackwell Science Inc., Oxford, U.K. 1–11.

Raposo, G., D. Tenza, D.M. Murphy, J.F. Berson, and M.S. Marks. 2001. Distinct protein sorting and localization to premelanosomes, melanosomes, and lysosomes in pigmented melanocytic cells. *J. Cell Biol.* 152:809–824.

Robinson, M.S. 2004. Adaptable adaptors for coated vesicles. *Trends Cell Biol.* 14:167–174.

Robinson, M.S., and T.E. Kreis. 1992. Recruitment of coat proteins onto Golgi membranes in intact and permeabilized cells: effects of brefeldin A and G protein activators. *Cell.* 69:129–138.

Romani de Wit, T., H.P. de Leeuw, M.G. Rondaij, R.T. de Laaf, E. Sellink, H.J. Brinkman, J. Voorberg, and J.A. van Mourik. 2003. Von Willebrand factor targets IL-8 to Weibel-Palade bodies in an endothelial cell line. *Exp. Cell Res.* 286:67–74.

Ruggeri, Z.M. 1999. Structure and function of von Willebrand factor. *Thromb. Haemost.* 82:576–584.

Sachse, M., S. Urbe, V. Oorschot, G.J. Strous, and J. Klumperman. 2002. Bilayered clathrin coats on endosomal vacuoles are involved in protein sorting toward lysosomes. *Mol. Biol. Cell.* 13:1313–1328.

Sadler, J.E. 1998. Biochemistry and genetics of von Willebrand factor. *Annu. Rev. Biochem.* 67:395–424.

Sakariassen, K.S., P.A. Bolhuis, and J.J. Sixma. 1979. Human blood platelet adhesion to artery subendothelium is mediated by factor VIII-Von Willebrand factor bound to the subendothelium. *Nature.* 279:636–638.

Simpson, F., A.A. Peden, L. Christopoulou, and M.S. Robinson. 1997. Characterization of the adaptor-related protein complex, AP-3. *J. Cell Biol.* 137:835–845.

Subramaniam, M., S. Saffaripour, L. Van De Water, P.S. Frenette, T.N. Mayadas, R.O. Hynes, and D.D. Wagner. 1997. Role of endothelial selectins in wound repair. *Am. J. Pathol.* 150:1701–1709.

Thiele, C., and W.B. Huttner. 1998. Protein and lipid sorting from the trans-Golgi network to secretory granules-recent developments. *Semin. Cell Dev. Biol.* 9:511–516.

Thomas, G. 2002. Furin at the cutting edge: from protein traffic to embryogenesis and disease. *Nat. Rev. Mol. Cell Biol.* 3:753–766.

Tooze, S.A., G.J. Martens, and W.B. Huttner. 2001. Secretory granule biogenesis: rafting to the SNARE. *Trends Cell Biol.* 11:116–122.

Ungewickell, E., H. Ungewickell, S.E. Holstein, R. Lindner, K. Prasad, W. Barouch, B. Martin, L.E. Greene, and E. Eisenberg. 1995. Role of auxilin in uncoating clathrin-coated vesicles. *Nature.* 378:632–635.

Urbe, S., M. Sachse, P.E. Row, C. Preisinger, F.A. Barr, G. Strous, J. Klumperman, and M.J. Clague. 2003. The UIM domain of Hrs couples receptor sorting to vesicle formation. *J. Cell Sci.* 116:4169–4179.

Voorberg, J., R. Fontijn, J. Calafat, H. Janssen, J.A. van Mourik, and H. Pannekoek. 1993. Biogenesis of von Willebrand factor-containing organelles in heterologous transfected CV-1 cells. *EMBO J.* 12:749–758.

Wagner, D.D. 1990. Cell biology of von Willebrand factor. *Annu. Rev. Cell Biol.* 6:217–246.

Wagner, D.D., J.B. Olmsted, and V.J. Marder. 1982. Immunolocalization of von Willebrand protein in Weibel-Palade bodies of human endothelial cells. *J. Cell Biol.* 95:355–360.

Wagner, D.D., S. Saffaripour, R. Bonfanti, J.E. Sadler, E.M. Cramer, B. Chapman, and T.N. Mayadas. 1991. Induction of specific storage organelles by von Willebrand factor propolypeptide. *Cell.* 64:403–413.

Waguri, S., F. Dewitte, R. Le Borgne, Y. Rouille, Y. Uchiyama, J.F. Dubremetz, and B. Hoflack. 2003. Visualization of TGN to endosome trafficking through fluorescently labeled MPR and AP-1 in living cells. *Mol. Biol. Cell.* 14:142–155.

Wasiak, S., V. Legendre-Guillemin, R. Puertollano, F. Blondeau, M. Girard, E. de Heuvel, D. Boismenu, A.W. Bell, J.S. Bonifacino, and P.S. McPherson. 2002. Enthoprotin: a novel clathrin-associated protein identified through subcellular proteomics. *J. Cell Biol.* 158:855–862.

Weibel, E.R., and G.E. Palade. 1964. New cytoplasmic components in arterial endothelia. *J. Cell Biol.* 23:101–112.